

Uplink MIMO Detection using Ising Machines: A Multi-Stage Ising Approach

Abhishek Kumar Singh¹, Ari Kapelyan³, Davide Venturelli², and Kyle Jamieson¹

¹*Department of Computer Science, Princeton University*

²*USRA Research Institute for Advanced Computer Science*

³*School of Applied and Engineering Physics, Cornell University*

Abstract

Multiple-Input-Multiple-Output (MIMO) signal detection is central to every state-of-the-art communication system, and enhancements in error performance and computation complexity of MIMO detection would significantly enhance data rate and latency experienced by the users. Theoretically, the optimal MIMO detector is the maximum-likelihood (ML) MIMO detector; however, due to its extremely high complexity, it is not feasible for large real-world communication systems. Over the past few years, algorithms based on physics-inspired Ising solvers, like Coherent Ising machines and Quantum Annealers, have shown significant performance improvements for the MIMO detection problem. However, the current state-of-the-art is limited to low-order modulations or systems with few users. In this paper, we propose an adaptive multi-stage Ising machine-based MIMO detector that extends the performance gains of physics-inspired computation to Large and Massive MIMO systems with a large number of users and very high modulation schemes (up to 256-QAM). We enhance our previously proposed delta Ising formulation and develop a heuristic that adaptively optimizes the performance and complexity of our proposed method. We perform extensive micro-benchmarking to optimize several free parameters of the system and evaluate our methods' BER and spectral efficiency for Large and Massive MIMO systems (up to 32 users and 256 QAM modulation).

I. INTRODUCTION

Multiple-Input-Multiple-Output (MIMO) signal detection is a key task in any modern wireless system. More than two decades of research have been dedicated to finding an efficient and practically feasible MIMO detector that can achieve good error performance. The optimal maximum-likelihood (ML) detector is known to be NP-Hard; hence the problem has an inherent

complexity-optimality trade-off: optimal performance requires exponential complexity for all known algorithms in the literature. Over the years, researchers have proposed several different methodologies and algorithms which populate the complexity-optimality spectrum for MIMO detection.

The invention of massive MIMO allowed practical systems to circumvent this complexity-optimality trade-off by having a larger number of receivers than the number of transmitters, leading to extremely well-conditioned channels. As a result, even linear detectors like Zero-Forcing (ZF) and Minimum Mean-Squared Error (MMSE) decoders could achieve near-optimal performance. However, this complexity reduction is not without trade-offs. Having less number of transmitters than receivers reduces the maximum throughput achievable by the cell and the number of users that can be served simultaneously. Therefore, developing an efficient MIMO detection algorithm that can achieve near-optimal performance will allow us to expand these massive MIMO systems into large MIMO systems and potentially improve the cell capacity [1].

Several conventional computation-based methodologies in the literature aim to achieve near-optimal MIMO detection with polynomial complexity. These methods rely on mathematical and algorithmic techniques like channel inversion, approximate tree-search [2], lattice reduction [3], successive interference cancellation [4] *etc.* However, their gains reduce drastically as the size of the MIMO system increases, or they require a significant increase in complexity to maintain performance, affecting their scalability for practical systems. This prompts us to explore alternative approaches for ML-MIMO detection that can provide scalable near-optimal MIMO detection for real-world systems.

Over the last few years, the use of machine learning and "Physics-inspired" computation for ML-MIMO has attracted the attention of researchers. While machine learning has shown remarkable results in several domains, the current state-of-the-art for ML-based systems has demonstrated its gains mostly in the Massive MIMO scenarios. While exploring ML-based solutions for near-optimal performance remains an interesting problem, we focus on the other alternative to conventional MIMO decoders: "Physics-inspired" computation.

The last five years have seen the rise of "Physics-inspired" computation methodologies as an alternative to conventional digital computation and have shown promising results for solving NP-Hard problems [5], [6]. These physics-inspired methods rely on creating a physical system whose dynamics embed the problem coefficients of an NP-Hard problem, and its steady state can be used to find the solution to the original problem. These physics-inspired methodologies include

Quantum Annealing [7], Coherent Ising Machines (optical or opto-electronic systems) [8], [9], [10], [11], [12], [13], and Oscillator-based Ising Machines [14].

Over the past few years, researchers have explored applications of physics-inspired computation for MIMO detection [15], [16], and have shown promising results. Several Quantum Annealing-based approaches, purely quantum[17] or classical-quantum hybrid [18], have been proposed and have shown significant performance gains for MIMO detection when low-order modulations (4-QAM and lower) are used. Researchers have also demonstrated performance improvements and near-optimal behavior for MIMO detection with other physics-inspired methodologies like Coherent Ising Machines [1] and Parallel Tempering [19]. However, the performance gains of all these methods are limited to low-order modulations like BPSK and 4-QAM, and their performance drastically reduces when higher-order modulations (16-QAM or higher) are used.

In the short conference version of this work [20], we proposed a novel Ising formulation, Delta Ising MIMO (DI-MIMO), of the maximum likelihood MIMO detection (ML-MIMO), which relies on searching for the optimal solution in a reduced search around an appropriately selected approximate solution. We demonstrate that it can provide significant performance gains for higher-order modulations (16-QAM to 256-QAM). In this paper, we improve upon DI-MIMO formulation and propose a multi-stage approach for MIMO detection. The main contributions of this paper are the following:

- 1) We improve the previously proposed delta-Ising [20] formulation for larger search radii, significantly enhancing the probability of success.
- 2) We propose a heuristic-based approach to adaptively determine the reduced search space for the ML-MIMO problem.
- 3) We propose a novel multi-stage MIMO decoding approach that iteratively adjusts the search space and the initial guess for the delta-Ising formulation, leading to significant performance improvements.

The rest of the paper is organized as follows: Section II describes the MIMO system model and the maximum likelihood (ML) MIMO detector. Section III is a primer on Coherent Ising machines (CIM) and describes the model used to evaluate our methods. Section IV describes our enhanced degenerate delta Ising formulation, a heuristic approach for estimating the required search radius (based on the channel measurements and received signal), and our Multi-Stage Delta Ising MIMO (MDI-MIMO) algorithm. Section V presents our evaluation results. We evaluate the

BER and spectral efficiency of our methods for 16×16 , 32×32 , 16×32 , and 32×64 MIMO systems. Our empirical analysis shows that our methods can provide significant performance improvements over MMSE-SIC [4] and the commonly used MMSE detector: achieving a BER of 10^{-3} (with 16-QAM and 64-QAM modulations) at an SNR approximately 4 dB lower than MMSE-SIC and 18 dB lower than MMSE, and providing throughput improvements (for large MIMO systems) of up to 100% over MMSE-SIC and up to 200% over MMSE. Even in the case of massive MIMO systems, where MMSE and MMSE-SIC are supposed to be near optimal, our methods can provide 50% better throughput. We perform extensive micro-benchmarking experiments to optimize the free parameters of our algorithm and justify our design choices. Finally, we evaluate our methods for a realistic 16×16 LTE scenario and demonstrate that our performance gains extend to realistic MIMO systems. We conclude our work and discuss some interesting future directions in Section VI.

II. SYSTEM MODEL

Consider an uplink MIMO Scenario with N_r antennas at the base station and N_t users with one transmit antenna each. This is equivalent to a $N_t \times N_r$ MIMO system and is described by a complex-valued $N_r \times N_t$ channel matrix $\tilde{\mathbf{H}}$. The symbol transmitted by each user is drawn from a fixed set Φ representing the M-QAM constellation. Let the transmit vector be $\tilde{\mathbf{x}}$ ($\tilde{\mathbf{x}} \in \Phi^{N_t}$), then the received vector $\tilde{\mathbf{y}}$ is given by

$$\tilde{\mathbf{y}} = \tilde{\mathbf{H}}\tilde{\mathbf{x}} + \mathbf{n}, \quad (1)$$

where \mathbf{n} is the channel noise. If the channel noise is assumed to be white Gaussian noise, then the maximum likelihood estimate for the transmitted vector $\tilde{\mathbf{x}}$ is given by

$$\tilde{\mathbf{x}}_{\text{ML}} = \arg \min_{\tilde{\mathbf{u}} \in \Phi^{N_t}} \|\tilde{\mathbf{y}} - \tilde{\mathbf{H}}\tilde{\mathbf{u}}\|^2. \quad (2)$$

Note that $\tilde{\mathbf{x}}$, $\tilde{\mathbf{y}}$ and $\tilde{\mathbf{H}}$ are all complex valued. Using the transform described in [1],

$$\mathbf{H} = \begin{bmatrix} \Re(\tilde{\mathbf{H}}) & -\Im(\tilde{\mathbf{H}}) \\ \Im(\tilde{\mathbf{H}}) & \Re(\tilde{\mathbf{H}}) \end{bmatrix}, \quad (3)$$

$$\mathbf{y} = \begin{bmatrix} \Re(\tilde{\mathbf{y}}) \\ \Im(\tilde{\mathbf{y}}) \end{bmatrix}, \quad \mathbf{x} = \begin{bmatrix} \Re(\tilde{\mathbf{x}}) \\ \Im(\tilde{\mathbf{x}}) \end{bmatrix}, \quad (4)$$

we get an equivalent real-valued problem,

$$\mathbf{x}_{\text{ML}} = \arg \min_{\mathbf{u} \in [\Re(\Phi)^{N_t}, \Im(\Phi)^{N_t}]} \|\mathbf{y} - \mathbf{H}\mathbf{u}\|^2. \quad (5)$$

In this paper, our objective is to efficiently solve (5) using a Coherent Ising Machine and get the solution to (2) by inverting the transform (4).

III. PRIMER: COHERENT ISING MACHINES

An Ising optimization problem [21] is a quadratic unconstrained optimization problem:

$$\arg \min_{\forall i, s_i \in \{-1, 1\}} - \sum_{i \neq j} J_{ij} s_i s_j = \min_{\mathbf{s} \in \{-1, 1\}^N} -\mathbf{s}^T \mathbf{J} \mathbf{s}, \quad (6)$$

where each *spin* variable $s_i \in \{-1, 1\}$, or in vector form (RHS) $\mathbf{s} = \{s_1, s_2, \dots, s_N\} \in \{-1, 1\}^N$, where the diagonal entries of the matrix \mathbf{J} are zeros. The Ising problem is known to be NP-Hard.

In an abstract way, we can think of an Ising machine as a system or algorithm that takes the coefficients of the Ising problem as the input and outputs a candidate solution to (6). While the Ising machine aims to find the global optimum, it can return a sub-optimal solution.

In this paper, we focus on Coherent Ising Machines (CIMs), but our methods can also be applied to other Ising machines. Coherent Ising machines were originally proposed ([9], [10], [11]) using an artificial optical spin network to find the ground state of the Ising problem.

The dynamics of several such bi-stable systems can be modeled with real-valued variables x_i such that the corresponding *spin* $s_i = \text{sign}(x_i)$. Given the Ising optimization problem

$$\arg \min_{s_1, s_2, \dots, s_N \in \{-1, 1\}} - \sum_{j \neq i} J_{ij} s_i s_j \quad (7)$$

The time evolution of such a system can be modeled using the ODE [22]

$$\forall i, \frac{dx_i}{dt} = (1 - p)x_i - x_i^3 + \epsilon \sum_{j \neq i} J_{i,j} x_j \quad (8)$$

Note that the CIM model used by RI-MIMO [1] can be approximated by (8) as well. However, the model described by (8) is susceptible to locally stable solutions (local minima of the Lyapunov function) and limit cycles [22], which can severely affect the likelihood of finding the ground state of (7). An enhanced model with an amplitude heterogeneity correction [22] can destabilize the local minima and avoid limit cycles. The amplitude heterogeneity correction-based model introduces new “error” variables e_i :

$$\forall i, \frac{dx_i}{dt} = (1 - p)x_i - x_i^3 + \epsilon e_i \sum_{j \neq i} J_{i,j} x_j \quad (9)$$

$$\forall i, \frac{de_i}{dt} = -\beta(x_i^2 - a)e_i, \quad e_i > 0, \quad (10)$$

where a, p , and β are the free parameters of the model. In [22], authors suggest that setting $p = 0.98$ and slowly ramping up ϵ with time t ($\epsilon = \gamma t$). a, β , and γ can be appropriately selected to maximize performance.

IV. DESIGN

A. Degenerate Delta-Ising Formulation

As noted in the short version of this work [20], the key idea of our proposed Delta Ising MIMO (DI-MIMO) methodology is to assume a guess for \mathbf{x}_{ML} in (5) and optimize to find the best correction to the guess, rather than optimizing to find \mathbf{x}_{ML} itself (unlike the existing state-of-the-art methods that use Quantum Annealing or CIMs).

We use the real-valued equivalent of the MMSE estimate (\mathbf{x}_m) as the guess. Note that this step has extremely low computation complexity and can be calculated from the MMSE solution using (4). Given the solution variable \mathbf{u} in the real-valued equivalent of the ML-MIMO problem (5), we define

$$\mathbf{d} = \mathbf{u} - \mathbf{x}_m, \quad (11)$$

where \mathbf{d} can be interpreted as the correction to the MMSE solution. The goal then becomes the formulation of an Ising problem for computing the optimal \mathbf{d} , such that $\mathbf{x}_m + \mathbf{d}$ will be the solution to (5). Note that, although we use the MMSE solution as the guess, any polynomial-time estimate of the MIMO problem (like FSD [2] or MMSE-SIC [4]) could be used as well.

For a QAM constellation, each element of \mathbf{d} corresponds to the difference between the real or imaginary parts of two QAM symbols and hence is an even-valued integer. The choice of the search space for \mathbf{d} is a design parameter; we can choose each element of \mathbf{d} to belong to the set $\mathcal{D}_1 = \{-2, 0, 2\}$, $\mathcal{D}_2 = \{-4, -2, 0, 2, 4\}$, or an even larger search space. The choice of the search space for \mathbf{d} reflects the region around the MMSE estimate that is searched for the optimal solution and determines the Delta Ising formulation. Let $\tilde{\mathbf{y}} = \mathbf{y} - \mathbf{H}\mathbf{x}_m$ be the residual received vector; then our new proposed formulation is obtained by substituting (11) in (5) to change the optimization variable to \mathbf{d} , and changing the search space to $\mathcal{D}_K^{2.Nt}$:

$$\hat{\mathbf{d}} = \arg \min_{\mathbf{d} \in \mathcal{D}_K^{2.Nt}} \|\tilde{\mathbf{y}} - \mathbf{H}\mathbf{d}\|^2. \quad (12)$$

The next step is to express \mathbf{d} using *spin* variables which can only take values -1 or 1 . Note that any scalar $c \in \{-2, 0, 2\}$ can be expressed using two *spin* variables $s_1, s_2 \in \{-1, 1\}$ as

$c = s_1 + s_2$. Similarly, if $c \in \{-4, -2, 0, 2, 4\}$ then it can be expressed using four *spin* variables as $c = s_1 + s_2 + s_3 + s_4$. Applying this reasoning for the vector \mathbf{d} , we can express \mathbf{d} as

$$\mathbf{d} = \mathbf{T}\mathbf{s}, \quad (13)$$

where \mathbf{T} denotes a transform matrix for $\mathcal{D}_K = \{-2K, -2K + 2, \dots, 2K\}$ for $K = 1, 2, \dots$, and \mathbf{s} is a $(4KN_t \times 1)$ spin vector (each element is ± 1).

$$\mathbf{T} = \mathbf{1}_{1 \times 2K} \otimes \mathbf{I}_{2 \cdot N_t} \quad (14)$$

Note that this degenerate delta Ising (dDI) transform differs from the delta Ising transform (DI) proposed in the short version [20], as for $K = 2$ ($\mathcal{D}_2 = \{-4, -2, 0, 2, 4\}$),

$$\mathbf{T} = \begin{cases} [2\mathbf{I}_{2 \cdot N_t} \ \mathbf{I}_{2 \cdot N_t} \ \mathbf{I}_{2 \cdot N_t}], & \text{delta-Ising: IEEE GLOBECOM '22 [20]} \\ [\mathbf{I}_{2 \cdot N_t} \ \mathbf{I}_{2 \cdot N_t} \ \mathbf{I}_{2 \cdot N_t} \ \mathbf{I}_{2 \cdot N_t}], & \text{degenerate delta-Ising: PROPOSED} \end{cases}. \quad (15)$$

We will see in Section V-D, that the proposed modification significantly improves the error performance.

We get the equivalent Ising formulation of (5) by substituting (13) in (12):

$$\hat{\mathbf{s}} = \arg \min_{\mathbf{s} \in \{-1, 1\}^{2 \cdot N_t}} -\mathbf{h}^T \mathbf{s} - \mathbf{s}^T \mathbf{J} \mathbf{s}, \quad (16)$$

$$\mathbf{J} = -\text{zeroDiag}(\mathbf{T}'\mathbf{H}'\mathbf{H}\mathbf{T}) = -\text{zeroDiag}(\mathbf{1}_{2K \times 2K} \otimes \mathbf{H}'\mathbf{H}), \quad (17)$$

$$\mathbf{h} = 2\mathbf{T}'\mathbf{H}'\mathbf{y} = \mathbf{1}_{2K \times 1} \otimes 2\mathbf{H}'\mathbf{y}, \quad (18)$$

where $\text{zeroDiag}(\cdot)$ sets the diagonal elements to zero and \otimes is the Kronecker product. We solve the obtained Ising problem (using an Ising machine) to get $\hat{\mathbf{s}}$, and then compute $\hat{\mathbf{d}} = \mathbf{T}\hat{\mathbf{s}}$ and $\mathbf{x} = \mathbf{x}_m + \hat{\mathbf{d}}$. Since some elements of \mathbf{x} can be outside the QAM constellation, we round \mathbf{x} to the nearest QAM symbol. Finally, we can get the maximum likelihood MIMO solution, $\tilde{\mathbf{x}}$ in (2), from \mathbf{x} by inverting the transform described in (4).

The Ising problem obtained in (16) has both linear and quadratic terms; however, as we saw in Section III, CIM requires an Ising problem with only quadratic terms. We use an auxiliary spin variable [1] to convert all linear terms in (16) to quadratic and define an auxiliary Ising problem:

$$(\bar{\mathbf{s}}, \bar{s}_a) = \arg \min_{\mathbf{s} \in \{-1, 1\}^{2N_t}, s_a \in \{-1, 1\}} -(\mathbf{h}^T \mathbf{s})_{s_a} - \mathbf{s}^T \mathbf{J} \mathbf{s}. \quad (19)$$

and the solution of (16) can be obtained from the solution of the auxiliary Ising problem [1] using the equation $\hat{\mathbf{s}} = \bar{\mathbf{s}} \times \bar{s}_a$. This allows us to solve (16) on the CIM.

We solve each problem on the amplitude heterogeneity correction-based CIM (described by (9) and (10)). Borrowing the terminology from the Quantum Annealing literature, we refer to each run on the CIM as an ‘‘anneal.’’ A standard practice is to run multiple anneals, for the same problem, to enhance the probability of finding the optimal solution. Hence, we run N_a anneals for each problem instance, *i.e.*, we solve each problem N_a times on the CIM and generate N_a candidate solutions. We compare the obtained candidate solutions and the initial guess and select the best solution based on the cost of the objective function in (5).

B. Search Space Estimation

The key idea of DI-MIMO is to find the optimal correction to the polynomial-time guess to reach the ground state. However, if the polynomial-time guess is already correct or very close to the optimal solution, we can skip DI-MIMO decoding. Further, the search space of the problem can be reduced by estimating the distance to the optimal solution. Therefore, having a mechanism to quantify the error in the initial guess can help us significantly reduce the computational load.

Consider the DI-MIMO problem given by (12),

$$\hat{\mathbf{d}} = \arg \min_{\mathbf{d} \in \mathcal{D}^{2 \cdot N_t}} \|\tilde{\mathbf{y}} - \mathbf{H}\mathbf{d}\|^2. \quad (20)$$

Note that $\mathbf{d} = 0$ corresponds to the initial guess. If a better solution exists, it implies

$$\exists \mathbf{d} : \|\tilde{\mathbf{y}} - \mathbf{H}\mathbf{d}\|^2 < \|\tilde{\mathbf{y}}\|^2 \quad (21)$$

$$\implies \exists \mathbf{d} : \mathbf{d}^T (\mathbf{H}^T \mathbf{H}) \mathbf{d} - 2(\tilde{\mathbf{y}}^T \mathbf{H}) \mathbf{d} < 0. \quad (22)$$

Since $(\mathbf{H}^T \mathbf{H})$ is a positive semi-definite matrix and has non-negative eigen values $(\lambda_1, \lambda_2 \dots \lambda_{2 \cdot N_T})$, by eigen-value decomposition $\mathbf{H}^T \mathbf{H} = \mathbf{Q}^T \mathbf{\Sigma} \mathbf{Q}$, where $\mathbf{\Sigma} = \text{diag}(\lambda_1, \lambda_2 \dots \lambda_{2 \cdot N_T})$. Further, since \mathbf{Q} is Unitary, $\|\mathbf{Q}\mathbf{d}\| = \|\mathbf{d}\| \geq K$, if \mathbf{d} has at-least one element equal to K .

$$\forall \mathbf{d} : \mathbf{d}^T (\mathbf{H}^T \mathbf{H}) \mathbf{d} - 2(\tilde{\mathbf{y}}^T \mathbf{H}) \mathbf{d} > \lambda_{\min} \|\mathbf{Q}\mathbf{d}\|^2 - 2\|\tilde{\mathbf{y}}^T \mathbf{H}\| \|\mathbf{d}\| \quad (23)$$

$$\implies \forall \mathbf{d} : \mathbf{d}^T (\mathbf{H}^T \mathbf{H}) \mathbf{d} - 2(\tilde{\mathbf{y}}^T \mathbf{H}) \mathbf{d} > \lambda_{\min} K^2 - 2\|\tilde{\mathbf{y}}^T \mathbf{H}\| K. \quad (24)$$

Therefore, if

$$\lambda_{\min} K - 2\|\tilde{\mathbf{y}}^T \mathbf{H}\| > 0 \implies \text{No solution with at least one element equal to } K \text{ exists.} \quad (25)$$

For a better solution (with at least one element equal to K) to exist, the necessary condition is given by

$$\frac{1}{K} < \frac{\lambda_{min}}{2\|\tilde{\mathbf{y}}^T\mathbf{H}\|}. \quad (26)$$

Therefore, let 2ω be the highest difference between the I/Q components of symbols drawn from some M -QAM modulation. For instance, $2\omega = 2$ for 4-QAM, $2\omega = 4$ for 16-QAM, and $2\omega = 14$ for 64-QAM. then for any $K < 2\omega$, if

$$\frac{1}{K} < \frac{\lambda_{min}}{2\|\tilde{\mathbf{y}}^T\mathbf{H}\|} \quad (27)$$

then for each element \hat{d}_i of $\hat{\mathbf{d}}$ in (12), $-K < d_i < K$. Further, since \hat{d}_i can only take even values, the appropriate search space can be given by, Let us define $\Gamma = \frac{2\|\tilde{\mathbf{y}}^T\mathbf{H}\|}{\lambda_{min}}$

$$\mathcal{D}_\omega = \{-2\omega, -2\omega + 2, \dots, 2\omega\}, \text{ if } 2\omega \leq \Gamma \quad (28)$$

else,

$$\mathcal{D}_R = \{-2R, -2R + 2, \dots, 2R\}, \text{ s.t } 0 \leq 2R < 2\omega \text{ and } \Gamma - 2 < 2R \leq \Gamma, \quad (29)$$

However, using λ_{min} leads to an extremely conservative metric, and we can relax this exact metric to a heuristics which uses λ_{mean} or λ_{max} instead of λ_{min} , *i.e.*, $\Gamma = \frac{2\|\tilde{\mathbf{y}}^T\mathbf{H}\|}{\lambda_{mean}}$ or $\Gamma = \frac{2\|\tilde{\mathbf{y}}^T\mathbf{H}\|}{\lambda_{max}}$. We will show in Section V-C, this procedure significantly reduces the computation load while having an acceptable impact on the performance (especially in mid-high SNR scenarios).

C. Multi-Stage Delta Ising-MIMO (MDI-MIMO)

In this section, we describe the proposed Multi-Stage-Delta-Ising-based MIMO detection (MDI-MIMO) algorithm. Given a MIMO instance and a budget of N_a total anneals, the MDI-MIMO algorithm (that allows S stages and explores at most R_{max} neighbours) is as follows:

- 1) Calculate the anneal budget for each stage $N_s = N_a/S$.
- 2) Set *current - stage* = 1.
- 3) Calculate the MMSE estimate (\mathbf{x}_m) and MMSE-SIC (\mathbf{x}_s) estimate of the MIMO problem.
- 4) set $\mathbf{x}_1 = \mathbf{x}_m$ and $\mathbf{x}_2 = \mathbf{x}_s$. These will serve as the initial guesses for DI-MIMO formulation.
- 5) Compute the appropriate search space around \mathbf{x}_1 . Let this be \mathcal{D}_{R_1} , such that $R_1 \leq R_{max}$ (if the computed R_1 is larger than R_{max} we set it equal to R_{max}). The idea is to create multiple parallel instances of DI-MIMO in each symmetric subset of \mathcal{D}_{R_1} . Therefore if $\mathcal{D}_{R_1} = \{-2R_1, \dots, 2R_1\}$, then we would create R_1 parallel instances of DI-MIMO in search spaces: $\{-2, 2\}, \{-4, 4\}, \dots, \{-2R_1, 2R_1\}$.

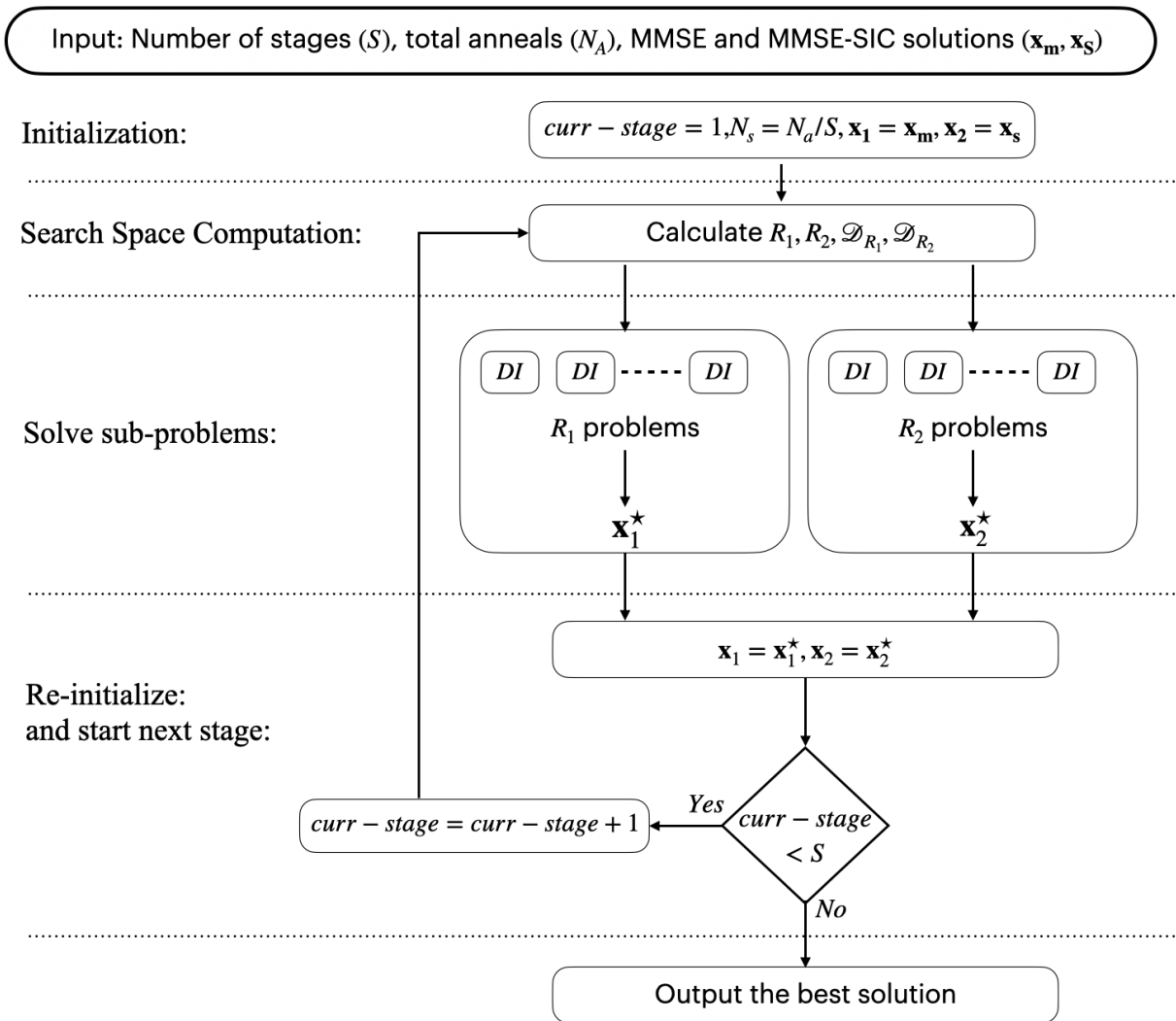


Fig. 1: MDI-MIMO: flow diagram illustrating various steps in the algorithm.

- 6) Repeat previous step, for \mathbf{x}_2 and compute R_2 .
- 7) Next we run each of the $(R_1 + R_2)$ DI-MIMO instances, computed in the last two steps with $N_s/(R_1 + R_2)$ anneals each.
- 8) From the R_1 and R_2 instances corresponding to \mathbf{x}_1 and \mathbf{x}_2 respectively, select the best solutions \mathbf{x}_1^* and \mathbf{x}_2^* .
- 9) If $current - stage = S$ go to step-10, otherwise set $\mathbf{x}_1 = \mathbf{x}_1^*, \mathbf{x}_2 = \mathbf{x}_2^*$, increment $current - stage$ by 1, and go to step-5.
- 10) Output the better solution out of \mathbf{x}_1^* and \mathbf{x}_2^* as the solution.

Note that, R_{max} can be interpreted as the maximum Chebyshev distance (L_∞ distance) to the

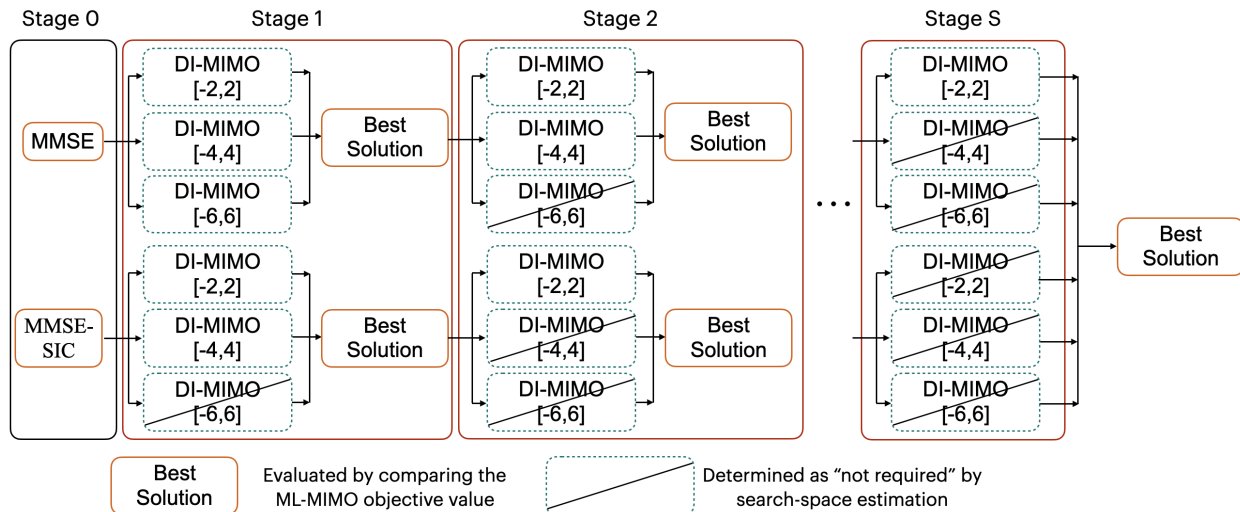


Fig. 2: MDI-MIMO: example execution for 16-QAM.

neighbors that MDI-MIMO wants to explore, and D_R corresponds to the search space involving neighbors that are at most R Chebyshev distance away from the initial guess.

V. EVALUATION

In this section, we evaluate our proposed algorithm for large and massive MIMO systems. We perform several benchmarking experiments to optimize the free parameters of our algorithm and justify our design choices. We further compute the BER and spectral efficiency of our methods for several MIMO systems with a large number of antennas and users. Finally, we demonstrate the performance of our methods in a realistic 3GPP-compliant LTE scenario.

A. Evaluation Setup

1) *Implementation of the CIM Simulator*: In this work, we implement an Ising solver by simulating the time evolution of the amplitude heterogeneity correction-based bi-stable system described by (9) and (10). Our simulator performs numerical integration using the Range-Kutta method (RK4) [23] for 512 time-steps and $dt = 0.005$. Note that the step size required for convergence of numerical integration will become increasingly smaller as the problem size increases. For the scenarios simulated in this paper, $dt = 0.005$ was found to be sufficient. The initial values x_i are i.i.d $\mathcal{N}(0, 0.001)$ and e_i are initialized using a folded $\mathcal{N}(0, 0.001)$ distribution. We set $p = 0.98$, $\beta = 1$, $a = 2$ and $\gamma = 1000/(256 \cdot 0.01)$. These parameters were empirically

selected, based on trial-and-error experiments, such that the system can achieve a steady state and attain good performance. Note that performance can be further improved by optimally selecting these parameters, and we plan to address this in our future work. If any iteration fails to converge in 512 integration steps, then the spin output \mathbf{s} is such that $\mathbf{T}\mathbf{s} = \mathbf{0}$ (where \mathbf{T} is the transform matrix defined by (14)).

2) *Evaluation Metrics*: Our evaluation setup simulates an uplink $N_t \times N_r$ MIMO system which has N_t users (with one transmit antenna each) and N_r receive antennas at the base station ($N_r > N_t$). We assume a slow-fading channel, and channel instances are assumed to follow the Rayleigh fading model. The BER is computed as the mean BER of all users. We compare our methods against MMSE-SIC with optimal ordering [4] and the MMSE detector in both large and massive MIMO scenarios. Spectral efficiency computations are based on convolutional coding with code-rates $\frac{1}{3}$, $\frac{1}{2}$, $\frac{2}{3}$, and an oracle Adaptive Modulation and Coding (AMC) module that selects the best modulation and code-rate based on SNR.

3) *Coupled-plots*: In this paper, we often use "coupled-plots" to describe several evaluation results. A coupled-plot between two entities (measured by same units) E_1 and E_2 , where data corresponding to E_1 is in sorted order, involves: plotting E_1 on the x-axis and the corresponding instance index on the y-axis (this is equivalent to a CDF of E_1 multiplied by the total number of instances). For each data point (representing an instance of E_1), the corresponding value of E_2 is indicated using an error bar. For readability of plots, the error bar is not plotted for every instance but for a smaller uniformly sampled subset of instances.

B. Performance Analysis

In this section, we emulate the end-to-end performance of several large MIMO and massive MIMO systems. We assume an oracle Adaptive Modulation and Coding (AMC) module, which can select the best modulation and coding scheme (among the available options) for every SNR. Such an oracle AMC allows us to approximate the spectral efficiency of the system empirically. We allow our system to use, 4-, 16-, 64-, and 256-QAM modulation and convolutional coding with $\frac{1}{3}$, $\frac{1}{2}$, and $\frac{2}{3}$. Since for 4-QAM we have shown DI-MIMO to be near optimal, we continue using it. The parameters for MDI-MIMO can be defined using a 4-tuple $(N_s, \text{heuristic}, R_{max}, S)$. We simulate our methods with the following parameters:

	4-QAM	16-QAM	64-QAM	256-QAM
	DI-MIMO	MDI-MIMO	MDI-MIMO	MDI-MIMO
16 × 16	(64, λ_{mean} , -, -)	(64, λ_{mean} , 3, 8)	(64, λ_{mean} , 4, 8)	(64, λ_{mean} , 8, 8)
32 × 32	(64, λ_{mean} , -, -)	(128, λ_{mean} , 3, 8)	(128, λ_{mean} , 4, 8)	(128, λ_{max} , 8, 8)
16 × 32	(64, λ_{mean} , -, -)	(8, λ_{mean} , 3, 8)	(8, λ_{mean} , 4, 8)	(8, λ_{mean} , 8, 8)
32 × 64	(64, λ_{mean} , -, -)	(8, λ_{mean} , 3, 8)	(8, λ_{mean} , 4, 8)	(8, λ_{mean} , 8, 8)

We choose λ_{max} heuristic for (32 × 32, 256-QAM) to reduce the execution time (see Section V-C), given the problem size is much higher at $R_{max} = 8$.

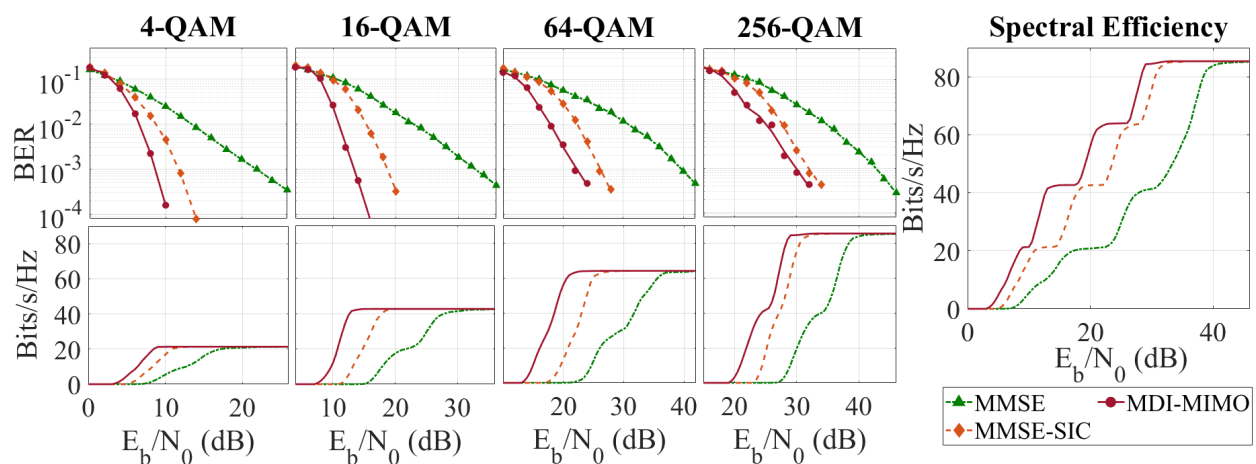


Fig. 3: BER and spectral efficiency performance of 16×16 Large MIMO: demonstrating that MDI-MIMO significantly outperforms both MMSE and MMSE-SIC and provides much higher spectral efficiency.

C. Analysis of search space estimation

In Section IV-B, we proposed a heuristic method to estimate the maximum required search space size for a problem instance. In this section, we will evaluate the error and complexity reduction of the proposed approaches. We simulate an 8×8 MIMO system, with MMSE-SIC as the initial guess for the dDI formulation, and evaluate the following:

- 1) %run-time = fraction of instances required to be solved on the CIM, *i.e.*, predicted search space size is greater than 0.
- 2) %wrong-prediction = fraction of instances for which the optimal solution lies outside the estimated search space.

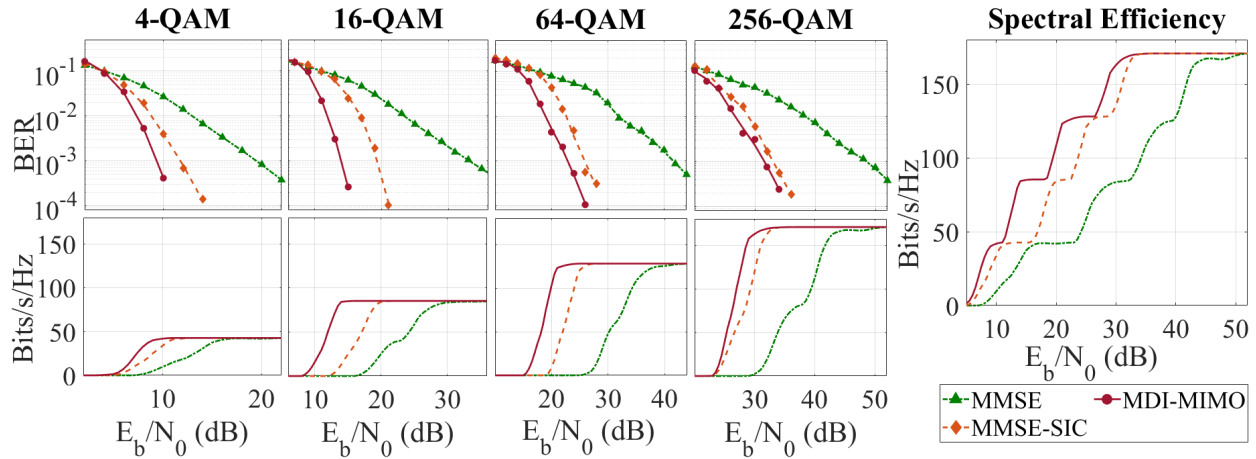


Fig. 4: BER and spectral efficiency performance of 32×32 Large MIMO: demonstrating that MDI-MIMO significantly outperforms both MMSE and MMSE-SIC and provides much higher spectral efficiency.

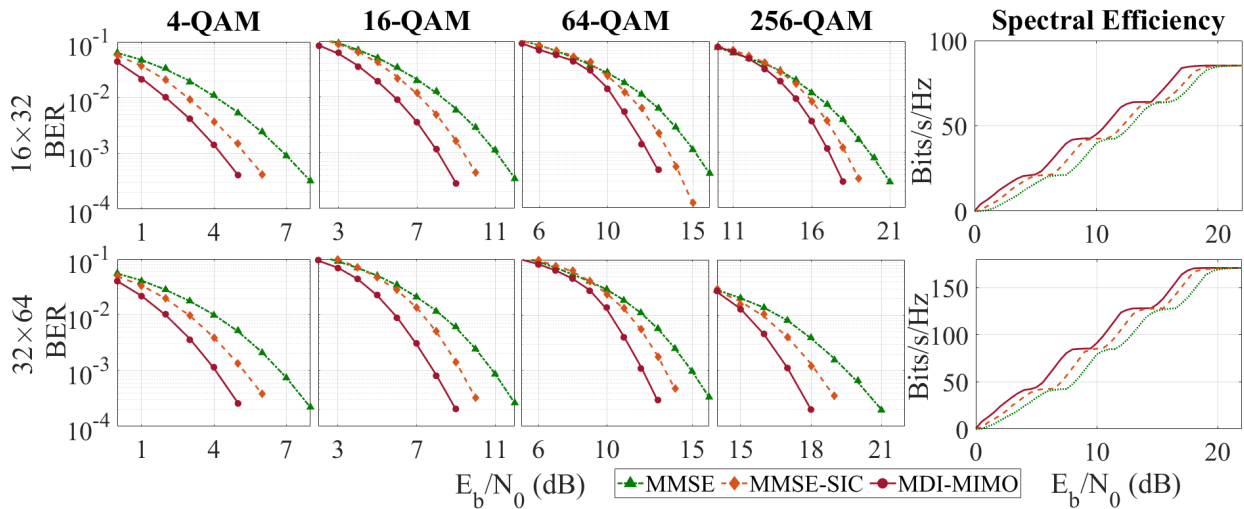


Fig. 5: BER and spectral efficiency performance of 16×32 and 32×64 Massive MIMO: demonstrating that MDI-MIMO significantly outperforms both MMSE and MMSE-SIC and provides much higher spectral efficiency.

Further, we evaluate both scenarios: use of maximum (λ_{max}) or mean (λ_{mean}) eigenvalue (of the real-equivalent channel) for search space estimation. We observe in Fig 6, both methods provide a significant reduction in the number of instances for which the Ising machine needs to be used, hence, drastically reducing the computational load on the Ising machine. While the prediction

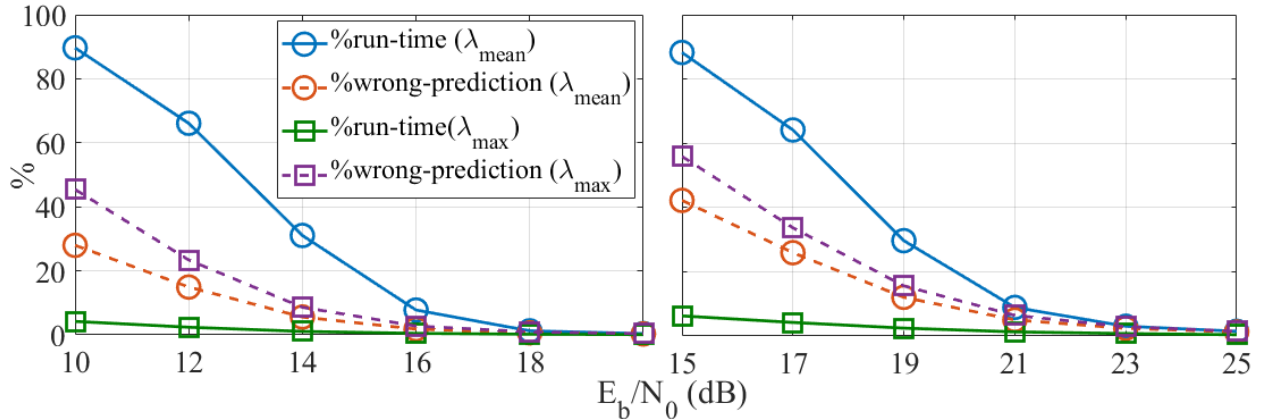


Fig. 6: Analysis of search space estimation heuristics for 8×8 MIMO system with 64-QAM modulation: demonstrating a significant reduction in the complexity with low prediction error, especially at mid-high SNR

error can be high at low SNR, it rapidly reduces and becomes very low for mid and high-SNR scenarios. We also note that using λ_{max} (compared to λ_{mean}) leads to a lower run-time at the cost of higher prediction error. In this paper, we use λ_{mean} for our evaluation due to its lower prediction error, unless specified otherwise.

D. Performance improvements due to degenerate delta Ising representation

As noted previously, In this paper we propose a modification to the delta Ising representation. While both these representations are equivalent for $\mathcal{D}_2 = \{-2, 0, 2\}$, for larger search space the representations differ and the proposed degenerate delta-Ising formulation performs much better. For example, the representation for \mathcal{D}_2 is given by:

$$\mathbf{T} = \begin{cases} [2\mathbf{I}_{2 \cdot N_t} \ \mathbf{I}_{2 \cdot N_t} \ \mathbf{I}_{2 \cdot N_t}], & \text{delta-Ising (DI)} \\ [\mathbf{I}_{2 \cdot N_t} \ \mathbf{I}_{2 \cdot N_t} \ \mathbf{I}_{2 \cdot N_t} \ \mathbf{I}_{2 \cdot N_t}], & \text{degenerate delta-Ising (dDI)} \end{cases}. \quad (30)$$

In Fig 7, we simulate the performance of searching around MMSE solution using DI and dDI formulation (16×16 , 16-QAM, 15dB). Our empirical analysis shows that the dDI formulation has a much higher probability of finding the global optimal. While for a few instances, DI formulation might perform better than dDI, for a much larger number of instances dDI formulation has significantly better performance.

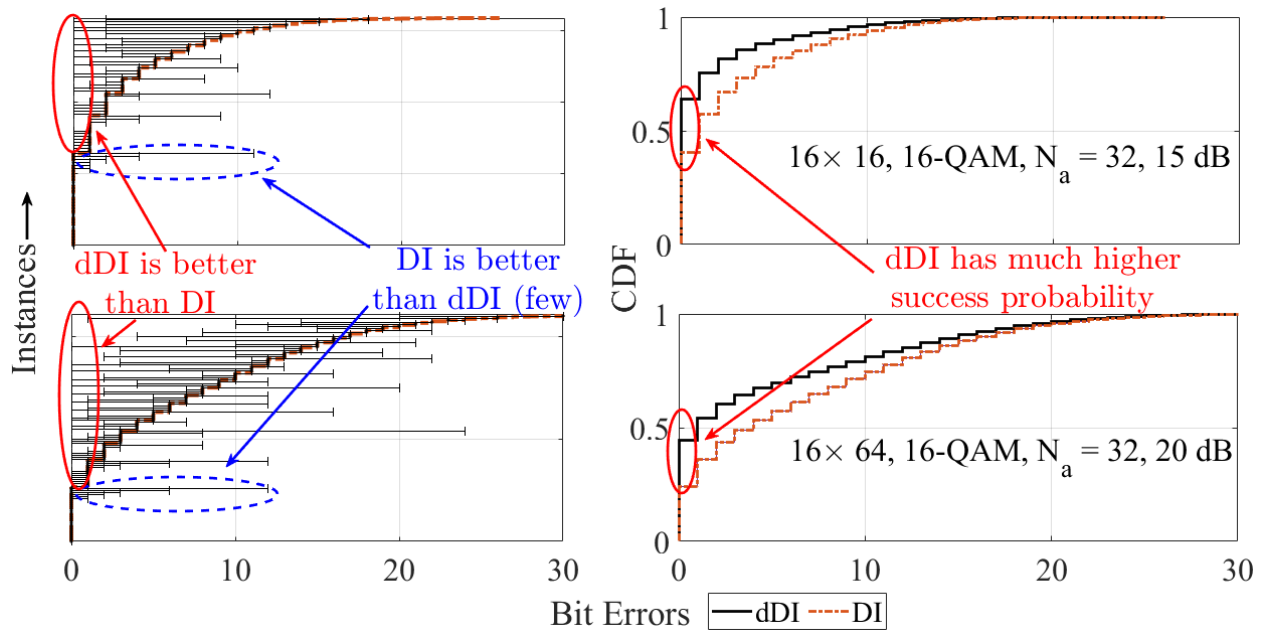


Fig. 7: Coupled-plot demonstrating bit errors for previously proposed DI and the improved dDI formulation for 16×16 , 64-QAM system: we see that dDI formulation leads to a much better overall probability of finding the ground state.

E. Why search in multiple search spaces?

In this section, we will empirically illustrate the necessity for multiple overlapping search spaces. We simulate at an $(8 \times 8, 16\text{-QAM})$ system and search around the MMSE-SIC solution using the dDI formulation for \mathcal{D}_1 and \mathcal{D}_2 (note that $\mathcal{D}_1 \subset \mathcal{D}_2$). We evaluate the 'coupled-plot' between the bit errors among the solutions obtained by searching in \mathcal{D}_1 and \mathcal{D}_2 . The underlying trade-off is the following: searching in \mathcal{D}_1 requires a lesser number of spin variables than \mathcal{D}_2 , therefore the problem is less complex, and it is easier for the Ising machine to find the ground state compared to searching in \mathcal{D}_2 (which can deteriorate the performance due to lower success probability). However, in the scenarios where the ground state is not in \mathcal{D}_1 , searching in \mathcal{D}_2 or larger is required. We see in Fig 8, for instances where the optimal solution is in \mathcal{D}_1 , search in \mathcal{D}_1 finds it with very high probability, and for several instances search in \mathcal{D}_2 performs worse. However, for the instances when optimal is not in \mathcal{D}_1 , CIM finds the optimal solution in \mathcal{D}_2 . Therefore, to cover both these scenarios and achieve the best performance, searching in multiple overlapping search spaces is required.

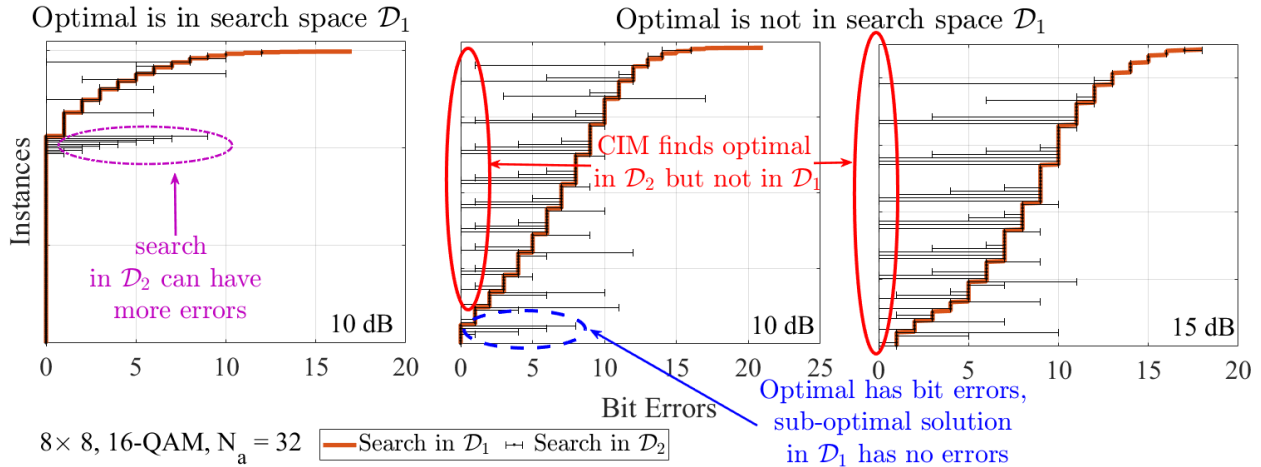


Fig. 8: Coupled-plot demonstrating bit errors obtained by searching in different search spaces using the dDI formulations for 8×8 , 16-QAM system: while \mathcal{D}_2 covers the entire constellation, searching in \mathcal{D}_1 leads to a better performance when the optimal is contained within \mathcal{D}_1 . However, for scenarios when optimal is not in \mathcal{D}_1 , a search in \mathcal{D}_2 is required. Therefore, in order to achieve the best performance, we should concurrently search over both \mathcal{D}_1 and \mathcal{D}_2 (even though $\mathcal{D}_1 \subset \mathcal{D}_2$)

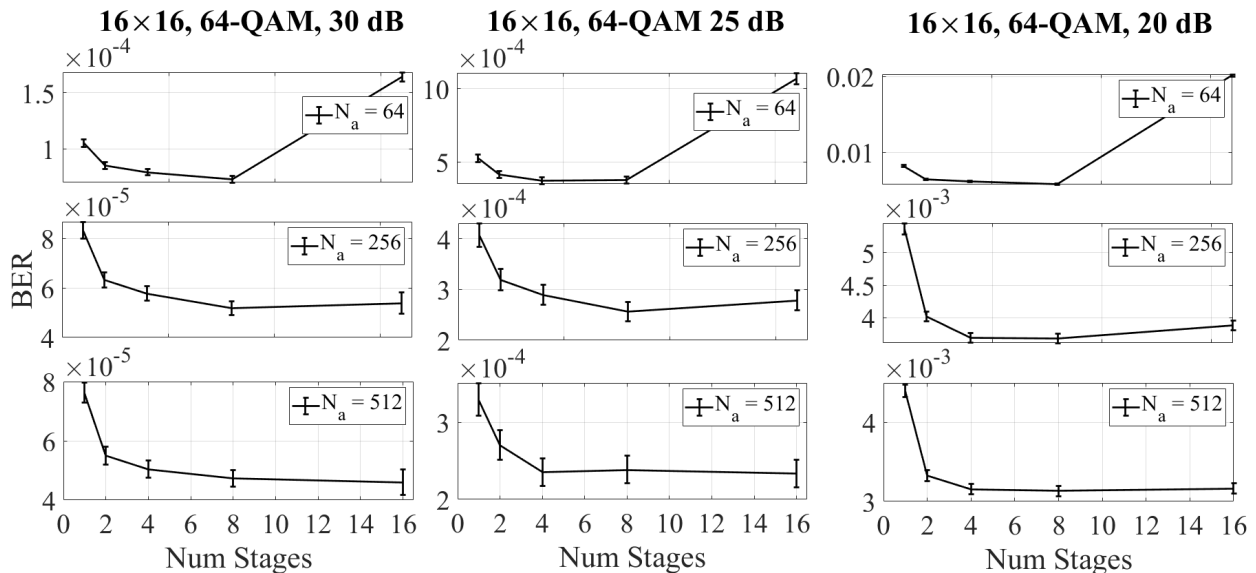


Fig. 9: Variation in the BER performance of MDI-MIMO algorithm with a different number of stages while keeping the total number of anneals fixed.

F. How many stages are required?

In this section, we benchmark the performance of MDI-MIMO *w.r.t* the number of stages (S). We simulate different scenarios in Fig 9, by fixing the total number of Anneals N_a . Given a fixed anneal budget N_a , if the number of stages is very high, the total number of anneals per stage is very low, and the performance of individual stages will be low; on the other extreme, if the number of stages is low, then the advantages of modifying the initial guess might be reduced. We observe similar trends in Fig 9, the performance initially improves with an increase in the number of stages and then starts deteriorating (as the number of anneals per stage reduces). Empirically we observe that $S = 8$ seems to provide the near-best performance.

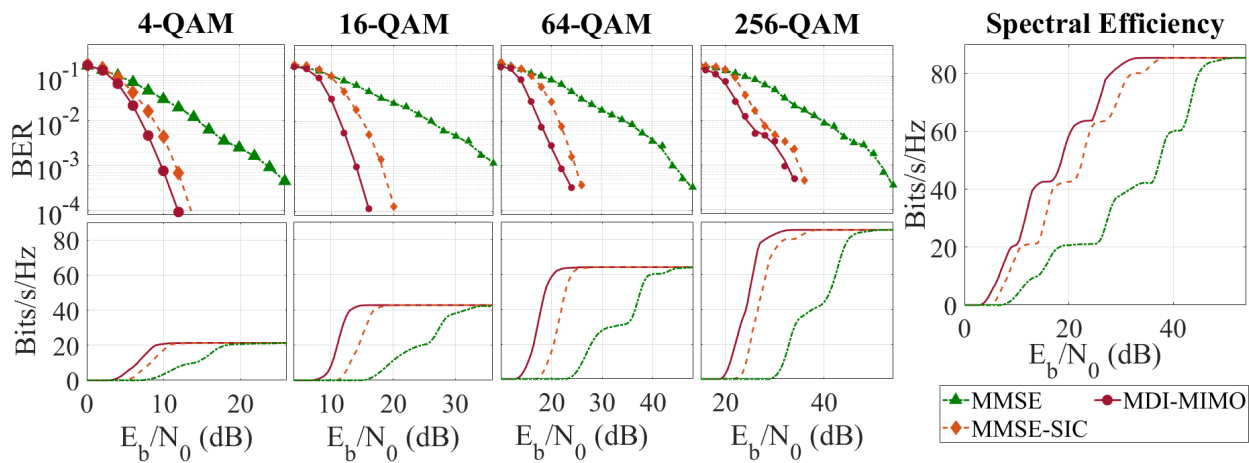


Fig. 10: BER and spectral efficiency performance of 16×16 Large MIMO on a more realistic channel model: demonstrating that MDI-MIMO significantly outperforms both MMSE and MMSE-SIC and provides much higher spectral efficiency.

G. Performance evaluation on more realistic channel model

In this section, we evaluate the performance of our methods over a realistic channel model. We use the Sionna simulator [24] to generate OFDMA channel traces corresponding to 3GPP Urban Macrocell (UMa) channel model. We use a single-sector topology with 16 users and a base station operating at 2.5 GHz, with 128 subcarriers and 15 KHz subcarrier spacing. The base station has 16 horizontally-polarized antennas arranged in a linear array. Each user is equipped with one horizontally polarized antenna. All users are moving at a speed of 3 m/s. All antennas have omnidirectional antenna patterns. This generates a 16×16 MIMO system. We report the

average BER over all users and all subcarriers. We see in Fig 10 that the previously observed performance gains with Rayleigh fading channels also extend to realistic MIMO scenarios. We observe that MDI-MIMO can significantly improve the performance of MMSE and MMSE-SIC, providing up to $2\times$ improvement in throughput over MMSE-SIC (up to $3\times$ over MMSE).

VI. CONCLUSION AND FUTURE WORK

In this paper, we propose our Multi-stage Delta Ising MIMO algorithm (MDI-MIMO) which performs an adaptive multi-stage search for the maximum likelihood solution of the MIMO problem using a Coherent Ising machine. MDI-MIMO can provide significantly improve the performance of MMSE and MMSE-SIC, and is the only known Ising machine-based algorithm in the literature (to the best of our knowledge) that can provide high-performance gains for 16-QAM or higher modulations in Large MIMO systems. Unlike its predecessor DI-MIMO which involves searching in a fixed search radius around an initial guess, MDI-MIMO can adaptively modify the initial guess and predict the appropriate search radius. This allows MDI-MIMO to significantly improve the performance gains, and deal with scenarios where the error in the initial guess is concentrated among a few users.

Through this work, we have been able to overcome the drawbacks of our predecessors RI-MIMO [1] (works only for 4-QAM or lower) and DI-MIMO [20] (limited performance gains due to fixed search radius), and have demonstrated our performance gains via simulations. As the next step, we plan to focus our efforts on building an FPGA/ASIC-based prototype of the CIM-based MIMO detector, and demonstrating that it can provide good quality solutions while meeting the timing/processing constraints of an LTE system.

REFERENCES

- [1] A. K. Singh, K. Jamieson, P. L. McMahon, and D. Venturelli, "Ising machines' dynamics and regularization for near-optimal mimo detection," *IEEE Transactions on Wireless Communications*, vol. 21, no. 12, pp. 11 080–11 094, 2022.
- [2] L. G. Barbero and J. S. Thompson, "Fixing the Complexity of the Sphere Decoder for MIMO Detection," *IEEE Transactions on Wireless Communications*, vol. 7, no. 6, pp. 2131–2142, 2008.
- [3] D. Wübben, D. Seethaler, J. Jalden, and G. Matz, "Lattice Reduction," *Signal Processing Magazine, IEEE*, vol. 28, pp. 70 – 91, 06 2011.
- [4] T.-H. Liu, "Some results for the fast mmse-sic detection in spatially multiplexed mimo systems," *IEEE Transactions on Wireless Communications*, vol. 8, no. 11, pp. 5443–5448, 2009.
- [5] Y. Haribara, S. Utsunomiya, and Y. Yamamoto, *A Coherent Ising Machine for MAX-CUT Problems: Performance Evaluation against Semidefinite Programming and Simulated Annealing*. Tokyo: Springer Japan, 2016, pp. 251–262.

- [6] S. Kawakami, Y. Mukasa, S. Bao, D. Ba, J. Arai, S. Yagi, J. Teramoto, and N. Togawa, "A constrained graph coloring solver based on ising machines," in *2023 IEEE International Conference on Consumer Electronics (ICCE)*, 2023, pp. 1–6.
- [7] P. Hauke, H. G. Katzgraber, W. Lechner, H. Nishimori, and W. D. Oliver, "Perspectives of quantum annealing: Methods and implementations," *Reports on Progress in Physics*, vol. 83, no. 5, p. 054401, 2020.
- [8] Z. Wang, A. Marandi, K. Wen, R. L. Byer, and Y. Yamamoto, "Coherent Ising machine based on degenerate optical parametric oscillators," *Physical Review A*, vol. 88, no. 6, p. 063853, 2013.
- [9] A. Marandi, Z. Wang, K. Takata, R. L. Byer, and Y. Yamamoto, "Network of time-multiplexed optical parametric oscillators as a coherent Ising machine," *Nature Photonics*, 2014.
- [10] P. L. McMahon, A. Marandi *et al.*, "A fully programmable 100-spin coherent Ising machine with all-to-all connections," *Science*, 2016.
- [11] T. Inagaki, Y. Haribara *et al.*, "A coherent Ising machine for 2000-node optimization problems," *Science*, vol. 354, no. 6312, pp. 603–606, 2016.
- [12] Y. Haribara, S. Utsunomiya, and Y. Yamamoto, "Computational Principle and Performance Evaluation of Coherent Ising Machine Based on Degenerate Optical Parametric Oscillator Network," *Entropy*, 2016.
- [13] F. Böhm, G. Verschaffelt, and G. Van der Sande, "A poor man's coherent Ising machine based on opto-electronic feedback systems for solving optimization problems," *Nature Communications*, vol. 10, 2019.
- [14] T. Wang and J. Roychowdhury, "OIM: Oscillator-Based Ising Machines for Solving Combinatorial Optimisation Problems," in *Unconventional Computation and Natural Computation*, I. McQuillan and S. Seki, Eds. Cham: Springer International Publishing, 2019, pp. 232–256.
- [15] M. Kim, S. Kasi, P. A. Lott, D. Venturelli, J. Kawell, and K. Jamieson, "Heuristic Quantum Optimization for 6G Wireless Communications," *IEEE Network (to appear)*, vol. 35, no. 4, 2021.
- [16] J. C. De Luna Ducoing and K. Nikitopoulos, "Quantum Annealing for Next-Generation MU-MIMO Detection: Evaluation and Challenges."
- [17] M. Kim *et al.*, "Leveraging Quantum Annealing for Large MIMO Processing in Centralized Radio Access Networks," *The 31st ACM Special Interest Group on Data Communication (SIGCOMM)*, 2019.
- [18] *Towards Hybrid Classical-Quantum Computation Structures in Wirelessly-Networked Systems*, 2020.
- [19] M. Kim, S. Mandra, D. Venturelli, and K. Jamieson, "Physics-Inspired Heuristics for Soft MIMO Detection in 5G New Radio and Beyond," in *Proceedings of the 27th Annual International Conference on Mobile Computing and Networking (MobiCom)*, 2021.
- [20] A. K. Singh, D. Venturelli, and K. Jamieson, "Perturbation-based formulation of maximum likelihood mimo detection for coherent ising machines," in *GLOBECOM 2022 - 2022 IEEE Global Communications Conference*, 2022, pp. 2523–2528.
- [21] A. Lucas, "Ising formulations of many NP problems," *Frontiers in Physics*, vol. 2, p. 5, 02 2014.
- [22] T. Leleu, Y. Yamamoto, P. L. McMahon, and K. Aihara, "Destabilization of local minima in analog spin systems by correction of amplitude heterogeneity," *Phys. Rev. Lett.*, vol. 122, p. 040607, Feb 2019.
- [23] D. Tan and Z. Chen, "On a general formula of fourth order runge-kutta method," *Journal of Mathematical Science & Mathematics Education*, vol. 7, no. 2, pp. 1–10, 2012.
- [24] J. Hoydis, S. Cammerer, F. Ait Aoudia, A. Vem, N. Binder, G. Marcus, and A. Keller, "Sionna: An open-source library for next-generation physical layer research," *arXiv preprint*, Mar. 2022.